Optics Communications ■ (■■■■) ■■■–■■■

Contents lists available at ScienceDirect

Optics Communications

journal homepage: www.elsevier.com/locate/optcom

Experimental and numerical study of a broad pass-band resonant optical metamaterials filter

Q1 M. Zhong [a,b], Y.H. Ye [a,*]

[a] Department of Physics, Nanjing Normal University, Nanjing 210023, China
[b] Hezhou College, Hezhou 542899, China

ARTICLE INFO

Article history:
Received 15 January 2015
Received in revised form
21 February 2015
Accepted 11 March 2015

Keywords:
Metamaterials
Pass-band
Surface plasmon polariton
Impedance match

ABSTRACT

A broad pass-band metamaterials-based optical filter is experimentally and numerically studied. The designed structure is constructed from a metal-dielectric-metal (MDM) sandwiched array. Measured results indicate that a broad pass-band can be achieved over 96.8% transmittance frequency range from 147.4 THz to 155.0 THz. Electrical field distributions indicate that the coupling and interaction between internal surface plasmon polariton (internal SPP) and localized surface plasmon (LSP) modes between silver layer and SU-8 layer leads to the broad pass-band. The influence of thickness of dielectric layer, the geometrical sizes of the cross hole (arm width W and arm length L) is experimentally examined. Finally, effects of variation of permittivity ε_d of dielectric layer are numerically surveyed. The compound structure metamaterials-based optical filter is demonstrated to have high tolerance to these parameters.

© 2015 Elsevier B.V. All rights reserved.

Q2

UNCORRECTED PROOF

1. Introduction

Metamaterials have attracted a great attention in recent years for unique electromagnetic propagation applications, due to their ability to offer a wide range of electromagnetic operations that are not available in natural materials [1–4]. The initial attention of researchers focus on comprehending rich optical phenomena of metamaterials and search the possibility of controlling electromagnetic waves through metamaterials devices. Then researchers are interested in exploiting and promoting various interesting applications in nano-fabrication and -detection, biochemical detection, integrated devices, and so on [5–12]. The recent studies on metamaterials based on nanofabricated metallic holes arrays and particle arrays gain enormous interest in a broad range of disciplines [13–16]. Moreover, there is a growing demand for pass-band metamaterials to ensure high tolerances well in multi-frequency operations in near infrared region. However, many pass-band metamaterials can't scale well. Actually, the specific geometry and arrangement of nano-scale inclusions that are typically aligned in a periodic lattice could influence the unique optical properties of these metamaterials [17]. The resonant properties of these inclusions would result in signal distortion and lead to narrow operational band-width [3,10], which leads to limit the application of these metamaterials in practical optical devices. It is known that the interaction and coupling of light with periodic metallic particle arrays or holes arrays can result in plasmon resonance. Moreover, electromagnetic resonant properties of optical metamaterials filter resulted by effective parameters (effective permeability, permittivity and refractive index) would lead to strong dispersive behavior across resonant band. This strong dispersive behavior therefore significantly limits the application of metamaterials-based optical filter in practical [18–20]. New strategies must be developed to tailor dispersive properties and increase the pass-band of metamaterials filter. In this paper, we proposed a novel structure metamaterials-based optical filter to modulate the dispersive behavior in resonance band, which consists of a metal-dielectric-metal (MDM) sandwich with a pair periodic slot metal structure and a dielectric layer. Measured results show that over 96.8% transmittance can be achieved across pass-band and the pass-bandwidth can be reached to 7.6 THz. Such a metamaterials-based optical filter could provide a desirable filtering mean to select targeted frequency band and thus lead to exploit most practical applications in the near infrared region.

2. Simulation methods and experimental details

The compound structure is shown in Fig. 1(a) and (b), each unit cell is constructed from a metal-dielectric-metal (MDM) sandwiched arrays. Metallic particles are separated by a 1.0 μm thick SU-8 [21] dielectric spacer. It should be noted that the dielectric layer is non-hollow. The metallic particle is selected to be silver in this paper and the relative dielectric function of silver layer follows the Drude model:

* Corresponding author.
E-mail address: yeyonghong@njnu.edu.cn (Y.H. Ye).

http://dx.doi.org/10.1016/j.optcom.2015.03.022
0030-4018/© 2015 Elsevier B.V. All rights reserved.

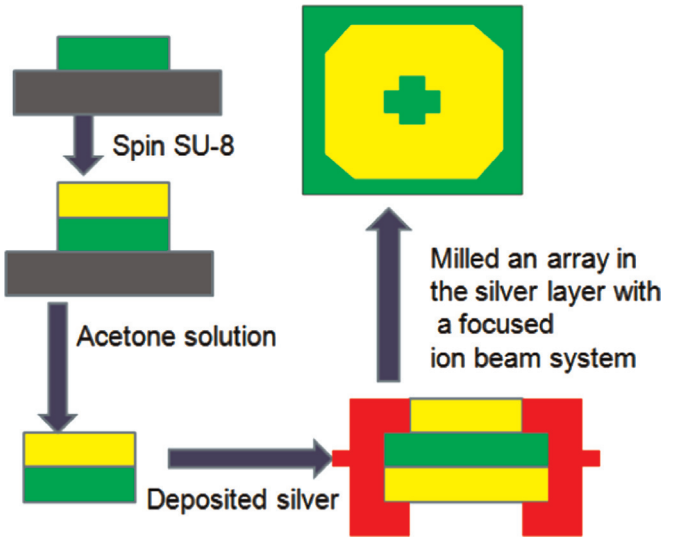

Fig. 1. (a) The top view of a unit cell; (b) the side view of a unit cell on the *xoz* plane. The yellow part is silver layer, and the green part is SU-8 dielectric layer. (c) Measured (black curve) and simulated (red curve) transmission spectra of samples. (d) SEMs of metamaterials-based optical filter samples. (For interpretation of the references to color in this figure legend, the reader is referred to the web version of this article.)

$$\varepsilon(\omega) = 1 - \frac{\omega_p^2}{\omega^2 - i\omega\gamma_D} \tag{1}$$

Here, $\omega_p = 1.37 \times 10^{16} s^{-1}$ is the plasma frequency, $\gamma_D = 9 \times 10^{13} s^{-1}$ is the collision frequency [22]. Dimensional parameters are shown in Table 1. To certify the designed structure which is discussed above, samples of the metamaterials-based optical filter are fabricated by using electron-beam lithography: first, spin a 1.0 μm thick layer of SU-8 onto a freestanding silicon wafer. Next, a silver layer is evaporated and deposited onto the upper surface of the SU-8 layer under 55e−10 (atm) working pressure. The metal- dielectric (MD) structure metamaterials is peeled off from the silicon wafer by soaked the MD metamaterials in acetone solution of lower concentration. Then, another silver layer is evaporated and deposited onto the other surface of the SU-8 layer under the same working pressure. Finally, an array of modified fishnet structure is milled in the top silver layer with a focused ion beam system [23] and then in the lower silver layer. A $3mm \times 3mm$large area samples is achieved to form a free-standing device. Images of samples are obtained by employed a JEOL JSM-5610LV SEM, as shown the inset in Fig. 1(d). Finally, transmittance spectra is measured at normal incidence (black curve) by employed a Bruker Optics Equinox 55 Fourier transform infrared spectrometer.

3. Optical properties of the broad pass-band filter

The compound structure is simulated through using Ansoft's HFSS 13.0 which is useful software in calculating periodic structure under vertical incidence [24]. This software is capable of wideband simulation of periodic structures with regular shape through considering only one unit cell of periodic structure. In our calculation, two ideal magnetic conductor planes are used on the boundary normal to the *x* axis, two ideal electric conductor planes are applied on the boundary normal to the *y* axis [25]. Bottom layer and top layer of the unit cell in Fig. 1(a)–(b) are assigned ideal conductor boundary, with conductivity equal to that of silver to simulate the silver ground plane. Fig. 1(c) shows measured (black curve) and simulated (red curve) transmission spectra. Two distinct transmission peaks can be observed at $f_1 = 147.4$ THzand $f_2 = 155.0$ THz in Fig. 1(c), which are named as "P_1 peak" and "P_2 peak" for the sake of convenience. In order to facilitate, we define $\Delta f = f_2 - f_1$ to characterize such a unique resonant pass-bandwidth [26–28], which is defined as the frequency range from f_1 (the lower-frequency point at which 95% energy transmits through the structure) to f_2 (the higher-frequency point at which 95% energy transmits through the structure) in this paper. Across the pass-band in Fig. 1(c), the average transmitted energy can be reached to 96.8% and the greatest variation of transmission energy is less than 3.4%. Such an optical metamaterials filter with so high value of pass-band is superior to previously reported structural metamaterials [29–32].

To get insight into the physical mechanism behind the transmission spectra in Fig. 1(c), the electrical field distribution on the *xoz* plane is also obtained and shown in Fig. 2(a)–(g). P_1 and P_2 peaks are associated with several resonance modes, as shown electric field distributions in Fig. 2(b) and (f). The resonance of external surface plasmon polariton (external SPP) mode on the lower surface of the lower silver layer, internal SPP mode between silver and SU-8 layers, localized surface plasmon (LSP) mode near edges of upper and lower silver layers can be observed obviously. Moreover, the coupling and interaction between internal SPP and LSP mode can be observed. With the resonance frequency near the center frequency of the pass-band, the intensity of external SPP mode is reduced, as shown in Fig. 2(c)–(e). On the contrary, the intensity of internal SPP and LSP are increased throughout the pass-band. Moreover, the intensity of the coupling and interaction between internal SPP and LSP modes (Fig. 2(c)–(e)) between silver layer and SU-8 layer is increased significantly. However, these coupling and interaction behaviors can't be found outside the pass-band, only external SPP mode can be observed obviously on the lower surface of the lower silver layer, as shown in Fig.2(a) and (g). These results indicate that the coupling and interaction between internal SPP and LSP modes between silver layer and SU-8 layer leads to the broad pass-band in Fig. 1(c).

The effect of thickness of dielectric layer on the pass-band is presented in Fig.3. With reduced *h2* from 1.0 μm to 0.7 μm, Δf is significantly expanded from 7.6 THz to 9.8 THz. However, the increase of pass-bandwidth is not linear. The lower thickness of dielectric layer can obtain a broader pass-band because of the dielectric layer characteristic impedance matches to free space

Table 1
All dimensional parameters of the compound structure.

Parameter	P	L L1	L2 W	h1	h2
Value(μm)	22	6 18	10 2	0.04	1

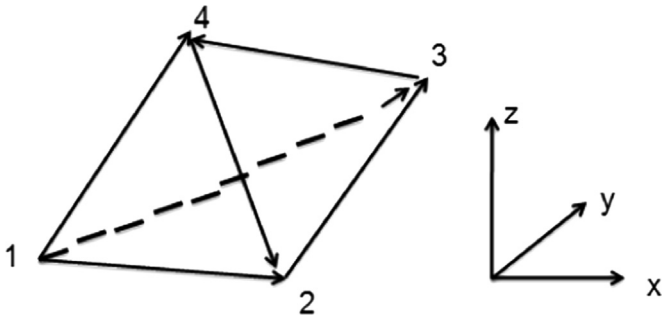

Fig. 2. Calculated density distributions of electric field is a part of the screenshots in *xoz* plane, correspond to the resonance frequency at (a)130.2 THz, (b)147.4 THz, (c)149.1 THz, (d)151.3 THz, (e)153.8 THz, (f)155.0 THz, (g)162.4 THz, respectively.

UNCORRECTED PROOF

Please cite this article as: M. Zhong, Y.H. Ye, Optics Communications (2015), http://dx.doi.org/10.1016/j.optcom.2015.03.022

Download English Version:

https://daneshyari.com/en/article/1533897

Download Persian Version:

https://daneshyari.com/article/1533897

Daneshyari.com